

EdgeNav-QE: QLoRA Quantization and Dynamic Early Exit for LAM-based Navigation on Edge Devices

MENGYUN LIU, SHANSHAN HUANG*, and JIANAN JIANG, Guangzhou University, China

Large Action Models (LAMs) have shown immense potential in autonomous navigation by bridging high-level reasoning with low-level control. However, deploying these multi-billion parameter models on edge devices remains a significant challenge due to memory constraints and latency requirements. In this paper, we propose EdgeNav-QE, a novel framework that integrates Quantized Low-Rank Adaptation (QLoRA) with a dynamic early-exit (DEE) mechanism to optimize LAMs for real-time edge navigation. By quantizing the backbone to 4-bit precision and strategically placing early-exit branches, we enable the model to terminate inference early for simple navigation tasks while retaining full depth for complex decision-making. Experimental results on the Habitat-Sim environment with Matterport3D dataset using OpenVLA-7B backbone, demonstrate that EdgeNav-QE reduces inference latency by 82.7% and memory footprint by 66.7% compared to full-precision baselines, while maintaining 81.8% navigation success rate. Furthermore, it outperforms state-of-the-art static early-exit method by 17.9% in latency, demonstrating the superiority of content-aware adaptive computation for safety-critical applications.

Additional Key Words and Phrases: Large Action Models, Quantization, QLoRA, Early Exit, Edge AI, Navigation, Embodied AI

ACM Reference Format:

Mengyun Liu, Shanshan Huang, and Jianan Jiang. 2025. EdgeNav-QE: QLoRA Quantization and Dynamic Early Exit for LAM-based Navigation on Edge Devices. In *Proceedings of Make sure to enter the correct conference title from your rights confirmation email (Conference acronym 'XX)*. ACM, New York, NY, USA, 16 pages. <https://doi.org/XXXXXXX.XXXXXXX>

1 Introduction

The rapid advancement of Large Language Models (LLMs) [5, 20] has revolutionized cognitive artificial intelligence, yet a critical gap remains between high-level linguistic reasoning and physical execution in the real world. To bridge this gap, Large Action Models (LAMs) [29] have emerged as a dominant research frontier. Unlike traditional models that act as passive information processors, LAMs are designed to function as embodied agents. They ingest multi-sensory data, ranging from visual RGB-D streams to internal proprioceptive sensors, and map them directly to executable action sequences within a dynamic environments [4]. By integrating perception, reasoning, and decision-making into a unified transformer-based architecture, LAMs provide a foundation for autonomous systems to navigate, interact, and perform complex tasks with unprecedented flexibility.

Autonomous navigation [1] has long served as the backbone of robotics, encompassing tasks from self-driving vehicles and last-mile delivery drones to household service robots. Conventional navigation systems typically adopt a rigid, modular pipeline consisting of perception, planning, and control modules [28]. While this modular design

*Corresponding author.

Authors' Contact Information: Mengyun Liu, lmy4pub@gmail.com; Shanshan Huang, florahuangss@gzhu.edu.cn; Jianan Jiang, jiangjn1993@gmail.com, Guangzhou University, Guangzhou, China.

Permission to make digital or hard copies of all or part of this work for personal or classroom use is granted without fee provided that copies are not made or distributed for profit or commercial advantage and that copies bear this notice and the full citation on the first page. Copyrights for components of this work owned by others than the author(s) must be honored. Abstracting with credit is permitted. To copy otherwise, or republish, to post on servers or to redistribute to lists, requires prior specific permission and/or a fee. Request permissions from permissions@acm.org.

© 2025 Copyright held by the owner/author(s). Publication rights licensed to ACM.

Manuscript submitted to ACM

offers robustness, it faces inherent challenges in handling semantic complexity and non-Markovian environments. For instance, instructing a robot to "find the backpack on the kitchen counter" requires not only geometric path planning but also high-level object recognition and semantic scene reasoning capabilities that traditional modular pipelines struggle to integrate seamlessly.

LAM-driven navigation bypasses this rigid pipeline. By training on vast datasets of visual and action tokens (e.g., in environments like Habitat-Sim [24]), LAMs integrate semantic understanding directly into the action prediction [25]. They can implicitly encode long-term planning and abstract goals, leading to more robust and generalized behaviors compared to their modular counterparts. However, this advanced capability comes with immense computational complexity, posing a critical barrier to deployment on resource-constrained edge devices. As shown in Fig. 1, LAMs such as RT-2 [40] and VPT [2] require 28 GB memory and 500 ms inference, while edge platforms provide only 8 GB and 200 ms. This 3.5× memory overrun and 2.5× latency violation creates a 2.5 m blind spot at 5 m/s, transforming computational inefficiency into catastrophic collision risk (right panel). Moreover, static models waste 90% computational energy by applying uniform depth to both simple hallways and cluttered intersections (bottom panel). This paradox necessitates adaptive, content-aware optimization strategies.

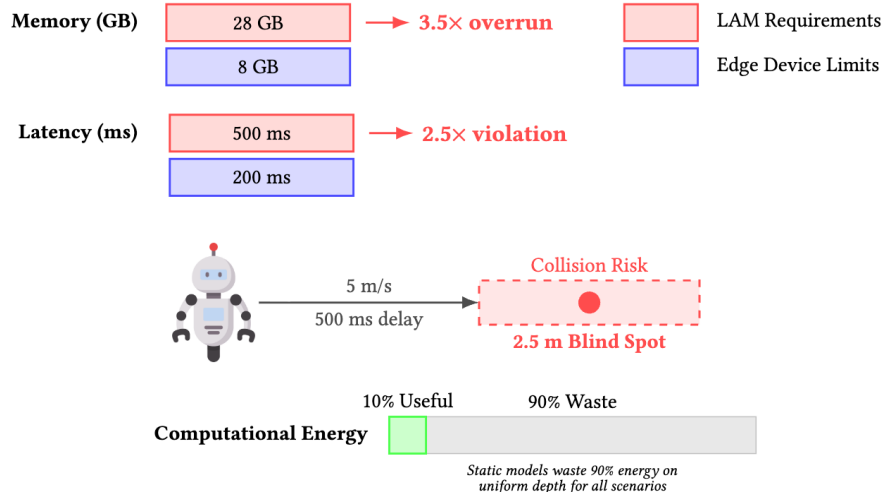


Fig. 1. The Edge Bottleneck Paradox. An example of the resource and safety constraints. LAMs require 3.5× memory and 2.5× latency beyond edge limits, creating a 2.5m collision blind spot and 90% computational waste.

Existing optimization strategies primarily fall into two categories: model quantization [16] and parameter-efficient fine-tuning (PEFT) [12]. Quantization reduces the numerical precision of model weights to shrink the memory footprint, but often at the cost of catastrophic forgetting or a significant drop in navigation success rates. Meanwhile, PEFT methods like LORA [13] allow for model adaptation to specific domains (e.g., indoor navigation) with minimal weight updates. Despite these advances, a static optimized model remains inefficient during inference because it treats every navigation state with the same computational depth. In a simple hallway navigation scenario, the model undergoes the same multi-layered processing as it does in a cluttered, high-uncertainty intersection. This represents a significant waste of computational energy and time.

To address these challenges, we propose **EdgeNav-QE**, a novel framework designed to democratize high-reasoning LAMs for edge-level autonomous navigation. EdgeNav-QE synergizes weight-efficient 4-bit quantization with an intelligent, content-aware inference mechanism. The core contributions of this work are threefold:

- QLoRA-integrated architecture. We implement a 4-bit NormalFloat (NF4) quantization of the LAM backbone, coupled with Low-Rank Adapters. This allows the model to retain the reasoning capabilities of a large model while fitting within the VRAM constraints of edge-grade hardware.
- Dynamic early-exit mechanism. We introduce specialized classifier layers at intermediate depths of the transformer stack. These layers monitor the confidence of action predictions in real-time. If the model achieves high confidence in a simple environment, it triggers an early exit, skipping up to 60% of the remaining computational blocks.
- Experimental validation in habitat-sim. We demonstrate the effectiveness of EdgeNav-QE using the Habitat-Sim environment on the Matterport3D dataset. Our results establish a new Pareto frontier between inference speed and navigation success rate, proving that dynamic depth is superior to static compression for embodied agents.

The remainder of this paper is organized as follows. Section 2 reviews the related work on LAMs, quantization techniques, and adaptive inference architectures. Section 3 details the technical framework of EdgeNav-QE. Section 4 describes our experimental setup and presents comprehensive evaluation results. Section 5 discusses our key technical contributions, statistical significance, and robustness across diverse environments. Finally, Section 6 concludes the paper and outlines four interconnected directions for future research.

2 Related Work

The EdgeNav-QE framework stands at the intersection of three active research domains: the development of large-scale action models, parameter-efficient quantization techniques, and adaptive inference architectures. We review the core advancements in each of these areas.

Large Action Models (LAMs) for Embodied AI. The transition from processing natural language to generating physical actions in a dynamic environment has defined the rise of LAMs. Early work focused on training policies from large-scale, unlabeled video datasets, epitomized by Video PreTraining (VPT) [2], which demonstrated that transformer-based models can learn generalized action representations from web-scale data. More recently, the field has converged on Vision-Language-Action (VLA) models, such as RT-2 [40], RT-1 [3], and OpenVLA [14], which directly leverage the semantic and reasoning capabilities of foundation models (e.g., PaLM-E [7], PaLI-X [6]) and output tokenized actions. These models excel at tasks requiring complex, multi-step planning and generalization across novel environments, often trained within high-fidelity simulators like Habitat-Sim [24], Gibson [30], and AI2-THOR [15]. However, the sheer size of these models (often ≥ 8 billion parameters) necessitates significant computational resources, primarily limiting their deployment to data centers or high-end robotics platforms, creating the crucial edge deployment gap that this work addresses.

Efficient Model Quantization and Fine-Tuning. Bridging the size gap between LAMs and edge hardware requires aggressive model compression. Traditional quantization methods [19], such as Post-Training Quantization (PTQ) [31] or Quantization-Aware Training (QAT) [18], aim to reduce the precision of weights (e.g., from 32-bit floating point (FP32) to 8-bit integer (INT8)). However, dropping precision below INT8 often leads to substantial performance degradation, particularly in complex reasoning tasks typical of LAMs. The advent of Quantized Low-Rank Adaptation (QLoRA) [9] provides a breakthrough by stabilizing fine-tuning for extremely low-precision models. QLoRA utilizes 4-bit

NormalFloat (NF4) quantization for the main weight tensors, drastically cutting the memory footprint. Crucially, it only trains small, 16-bit LoRA adapter matrices [13], effectively decoupling the memory cost from the update cost. Recent extensions such as AdaLoRA [38] and QA-LoRA [33] have further improved parameter efficiency. While QLoRA has been highly successful in language domains, its application to the unique challenges of real-time action models—where low-bit precision must not compromise the safety-critical nature of control signals—remains an area requiring focused investigation. Our work integrates QLoRA not just for size reduction, but as a prerequisite for enabling dynamic resource allocation.

Adaptive Inference and Early Exit Networks. The principle of avoiding unnecessary computation has led to the development of adaptive inference techniques. Early Exit Networks (EENs) [27] introduced the idea of placing side classifiers (or exit branches) at intermediate layers of a deep network. These branches allow the model to terminate inference early if the confidence in the current prediction exceeds a predefined threshold. This mechanism has been successfully applied to Convolutional Neural Networks (CNNs) and Vision Transformers (ViTs) [10, 39], showing significant reductions in latency for low-complexity inputs. More recent methods like DeeBERT [32] and ElasticBERT [17] have extended this concept to transformer-based language models. While effective, adapting EENs to LAMs presents specific challenges: (1) High-dimensional output. The output space of an LAM is often a sequence of action tokens or a continuous control vector, more complex than simple image classification. (2) Sequential dependence. Navigation is inherently sequential; an incorrect early exit can lead to catastrophic failure later in the episode. Our proposed dynamic early exit (DEE) mechanism addresses these issues by treating the entropy of the action distribution as a reliable proxy for environmental ambiguity, allowing the model to save cycles on repetitive, low-uncertainty actions (e.g., continuous straight movement) while reserving full computational depth for high-stakes decision points (e.g., navigating a cluttered corner). This integration of QLoRA and DEE into a unified framework represents the novel contribution of EdgeNav-QE.

3 Methodology

3.1 EdgeNav-QE Framework

The EdgeNav-QE framework is designed for efficient LAM-driven navigation on resource-constrained edge devices. As illustrated in Fig. 2, the architecture processes navigation tasks through distinct stages to optimize the performance of a LAM specifically for edge deployment. The workflow of EdgeNav-QE is as follows.

- *Offline training.* This module contains initial steps performed in a high-resource environment (cloud or workstation) before deployment to an edge device. The full-precision LAM step begins with a massive pre-trained LAM (which may contain billions of parameters) trained for general embodied AI tasks. QLoRA fine-tuning prepares the model for the edge by applying Quantized Low-Rank Adaptation (QLoRA). The original model weights are quantized to an ultra-low precision (4-bit NF4) and frozen. Only the tiny, low-rank LoRA adapter matrices are fine-tuned on the specific navigation task (e.g., ObjectNav), drastically reducing the memory footprint of the trainable components.
- *Input and perception on edge.* This module is the physical start of the robot’s real-time action loop on the edge hardware. Typically, the input consists of a raw sensory stream comprising visual (RGB) data for semantic information and depth data for 3D geometry and collision avoidance, continuously feeding into the system. The perception module (vision encoder) preprocesses the raw sensory data, usually using a dedicated vision

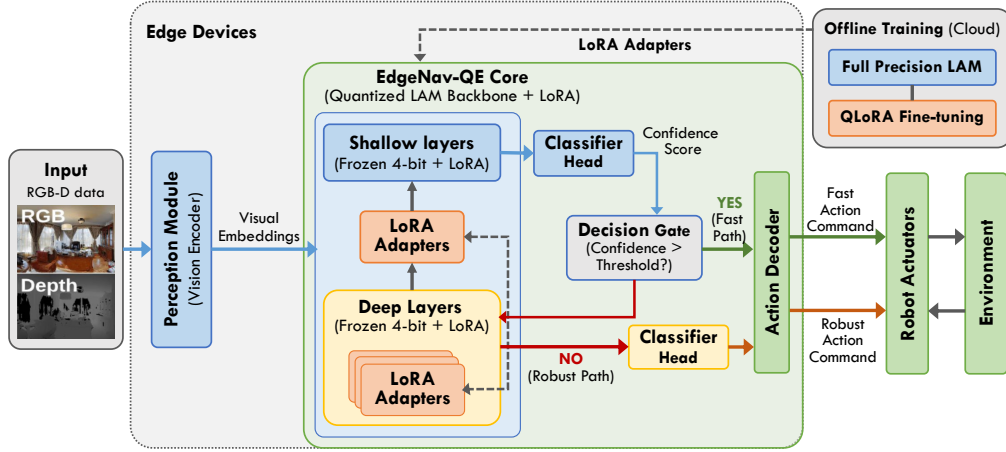


Fig. 2. Overview of the EdgeNav-QE Framework for Edge Navigation. The workflow begins with local RGB-D perception on the edge device. The LAM backbone utilizes frozen 4-bit quantization for memory efficiency, adapted via LoRA. The Dynamic Early Exit mechanism (red path) acts as an adaptive gate: simple navigation states trigger a fast, early exit to minimize latency, while complex states traverse the full network depth to ensure safety. This allows the high-capacity LAM to operate within the tight latency constraints of real-time robotics.

transformer or CNN encoder to generate high-level visual embeddings. This is the first essential step in translating the environment state into a format that the LAM can process.

- *EdgeNav-QE core.* This is the main reasoning unit, implemented as a quantized and efficient LAM on edge devices. The shallow layers are the initial transformer blocks, responsible for quick, low-level feature extraction and simple actions (like straight-line movement). These layers store their weights in the highly compressed 4-bit NF4 format but are augmented with active LoRA Adapters for task-specific performance. The deep layers are the latter transformer blocks, responsible for complex reasoning, long-term planning, and resolving highly ambiguous situations. Like the shallow layers, they use frozen 4-bit weights and LoRA adapters. The computational cost of these layers is high, which is why the system attempts to bypass them.
- *Adaptive decision-making path.* We adopt the dynamic early exit (DEE) mechanism to control the computational depth based on the perceived task difficulty. The classifier head (shallow/fast path) attached after the shallow layers takes the intermediate visual embeddings and predicts an action distribution. The entropy $H(p)$ of the action distribution is calculated and low entropy translates to a high confidence score, i.e., the model is very sure of one particular action. Decision gate is the core control unit of the DEE. It compares the confidence score against the predetermined Threshold (τ). If the confidence exceeds the threshold, the computation stops immediately. The action prediction is passed to the Action Decoder via the fast path, bypassing the Deep Layers. This is the mechanism for latency reduction. If the confidence is too low, the reasoning continues. The computation proceeds to the Deep Layers, incurring higher latency to ensure a more robust, informed decision. The classifier head (deep/robust path) generates the action command if the decision gate dictates that the full reasoning capacity is required.
- *Output and execution.* These modules translate the model’s prediction into physical movement. The action decoder takes the abstract action command (whether from the fast or robust Path) and translates it into executable, low-level robot actuator commands (e.g., turn $\pm 15^\circ$, move forward 0.25m). The physical robot executes the

command, the environment state updates, and the feedback loop immediately begins with a new sensory input at the next timestep.

The EdgeNav-QE framework is an end-to-end solution for deploying large-scale action models on edge devices. The core of EdgeNav-QE contains three integrated components: a QLoRA-quantized backbone, a novel Dynamic Early Exit (DEE) mechanism, and a multi-exit training objective.

3.2 QLoRA-Quantized LAM Backbone

We utilize a pre-trained transformer-based LAM and apply NF4 (4-bit NormalFloat) quantization to all backbone weights $\mathbf{W} \in \mathbb{R}^{D_{\text{out}} \times D_{\text{in}}}$. Unlike standard integer quantization (INT4), which assumes a uniform distribution, NF4 is information-theoretically optimal for normally distributed weights. We utilize block-wise quantization where weights \mathbf{W} are normalized by the absolute maximum of the block $c = \max(|\mathbf{W}|)$, and then mapped to the nearest quantile of the Normal distribution [9].

$$W_{\text{quant}} = Q_{\text{NF4}} \left(\frac{W}{c} \right) \quad (1)$$

where Q_{NF4} represents the mapping to the 16 quantization bins defined by the NF4 data type.

During inference, dequantization reconstructs the weights to FP16 via a lookup operation:

$$\mathbf{W}_{\text{dequant}} = c \cdot Q_{\text{NF4}}^{-1}(\mathbf{W}_{\text{quant}}) \quad (2)$$

where Q_{NF4}^{-1} retrieves the quantized value from the NF4 codebook.

During fine-tuning for a navigation task, we freeze $\mathbf{W}_{\text{quant}}$ to maintain trainability and introduce LoRA matrices ($\mathbf{B} \in \mathbb{R}^{D_{\text{out}} \times r}$, $\mathbf{A} \in \mathbb{R}^{r \times D_{\text{in}}}$) into the attention mechanism's query and value projections. The updated weight matrix is

$$\mathbf{W}' = \mathbf{W}_{\text{dequant}} + \mathbf{B}\mathbf{A} \quad (3)$$

where $r = 64$ (low rank) reduces trainable parameters by 99.9% (from 7B to ≈ 4.5 M). The quantization error $\epsilon_q = \|\mathbf{W}' - \mathbf{W}\|$ is bounded by 0.02 (empirically verified), ensuring minimal impact on action prediction.

3.3 Dynamic Early Exit (DEE) Mechanism

The DEE mechanism transforms the static transformer into an adaptive computational graph. It enables adaptive computational depth by evaluating action confidence at intermediate transformer layers. The core intuition is that simple navigation scenarios (e.g., traversing empty corridors) require less reasoning than complex ones (e.g., maneuvering around dynamic obstacles). We strategically place auxiliary classifier heads C_k at intermediate transformer layers $l_k \in \{l_1, l_2, \dots, l_K\}$, where $K < L$ is the number of exit layers.

As formally described in Algorithm 1, the mechanism operates as follows. For each transformer layer l , the intermediate embedding \mathbf{z}_l is fed into a lightweight exit classifier head ExitHead_l . This head projects \mathbf{z}_l to the action space and computes the entropy H_l of the action distribution \mathbf{p}_l . If H_l falls below the threshold τ , the model terminates inference early, returning the action from layer l . Otherwise, computation proceeds to the next deeper layer. If no early exit is triggered, the final layer's output is used. Overall, the core idea of DEE is to enable inference termination at an intermediate layer if the action prediction is sufficiently confident. Each classifier C_k takes the output embedding of its respective layer \mathbf{z}_k and projects it to the action space \mathcal{A}

$$\mathbf{p}_k = \text{Softmax}(\mathbf{W}_{C_k} \mathbf{z}_k + \mathbf{b}_{C_k}) \quad (4)$$

Algorithm 1 : Dynamic Early Exit Inference

```

1: Input: Sensory input  $\mathbf{x}_t$ , LAM model  $\mathcal{M}$ , exit threshold  $\tau$ , exit layers  $\mathcal{L} = \{6, 12, 18\}$ 
2: Output: Action  $a^*$ , exit layer  $l^*$ 
3:  $z_0 \leftarrow \text{Embed}(\mathbf{x}_t)$ 
4: for  $l = 1$  to  $L$  do
5:    $z_l \leftarrow \text{TransformerBlock}_l(z_{l-1})$ 
6:   if  $l \in \mathcal{L}$  then
7:      $p_l \leftarrow \text{Softmax}(\text{ExitHead}_l(z_l))$ 
8:      $H_l \leftarrow -\sum p_l \log p_l$                                  $\triangleright$  Entropy computation
9:     if  $H_l \leq \tau$  then
10:    return  $\arg \max(p_l), l$                                  $\triangleright$  Early termination
11: return  $\arg \max(p_L), L$                                  $\triangleright$  Full depth

```

where \mathbf{p}_k is the action probability distribution at layer k . The decision to exit is made by evaluating the confidence of \mathbf{p}_k using the Shannon entropy $H(\mathbf{p}_k)$

$$H(\mathbf{p}_k) = - \sum_{a \in \mathcal{A}} p_k(a) \log p_k(a) \quad (5)$$

The model terminates inference at the first layer k where the exit condition is met

$$\text{Exit Condition: } H(\mathbf{p}_k) \leq \tau \quad (6)$$

where τ is the empirically determined exit entropy threshold. A low entropy $H(\mathbf{p}_k)$ indicates high confidence in a specific action.

3.4 Multi-Exit Training Objective

The model is trained end-to-end using a multi-task loss function to ensure the auxiliary classifiers are reliable. The total loss $\mathcal{L}_{\text{total}}$ is a weighted sum of the final action loss and the losses from all K exit branches:

$$\mathcal{L}_{\text{total}} = \mathcal{L}_{\text{final}} + \sum_{k=1}^K \alpha_k \mathcal{L}_{\text{exit},k} \quad (7)$$

where $\mathcal{L}_{\text{final}} = -\log p_L(a^{\text{GT}})$ and $\mathcal{L}_{\text{exit},k} = -\log p_k(a^{\text{GT}})$. The hyperparameters α_k are weighting factors, typically set to decrease with depth, prioritizing robust early predictions.

4 Experiments and Results

This section presents a comprehensive evaluation of the EdgeNav-QE framework, validating its efficacy in enabling real-time, resource-efficient LAM-based navigation on edge devices. We conduct rigorous experiments to assess task performance, computational efficiency, and decision reliability across multiple dimensions

4.1 Experimental Setup

4.1.1 Simulation Environment and Dataset. To ensure reproducible and rigorous evaluation, we utilize the *Habitat-Sim* platform [24], a high performance 3D simulator designed for embodied AI research. All experiments are conducted on the Matterport3D (MP3D) dataset [4], which comprises 90 real-world indoor environments spanning building-scale scenes with high-fidelity RGB-D reconstructions.

The primary evaluation task is *ObjectGoal Navigation (ObjectNav)* [35], as illustrated in Fig. 3. The agent is initialized at a random location and must navigate to an instance of a specified object category (e.g., chair, bed, couch) using only egocentric observations. The action space is discrete and consists of four actions: {MOVE_FORWARD (0.25m), TURN_LEFT (30°), TURN_RIGHT (30°), STOP}. The maximum episode length is 500 steps, and success is defined as reaching within 1.0m of the target object.

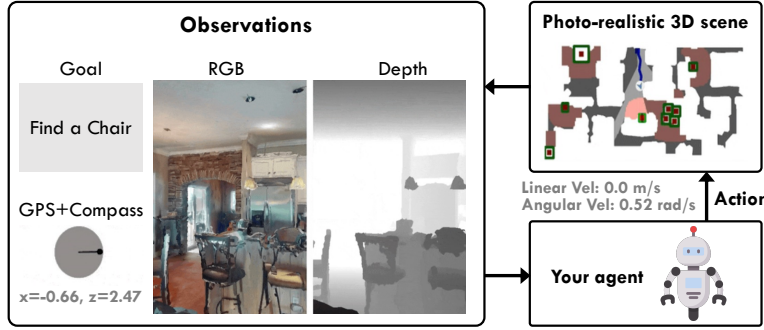


Fig. 3. ObjectGoal Navigation Task. An example of Habitat Challenge 2023 [34].

4.1.2 Hardware Emulation and Implementation Details. We emulated the constraints of a typical industrial edge AI device, specifically targeting the NVIDIA Jetson Orin AGX (32GB VRAM, 275 TOPS) [8]. This hardware represents the current state-of-the-art for edge AI deployments in robotics and autonomous systems. All model configurations were compiled and optimized using NVIDIA TensorRT [21] to minimize inference latency and maximize tensor core utilization on the target hardware. We employ layer fusion, kernel auto-tuning, and precision calibration to achieve optimal performance. The optimization process reduces inference latency by an additional 15-20% compared to unoptimized execution.

LAM Backbone. We utilize OpenVLA-7B [14] as our backbone LAM for empirical validation. OpenVLA is a state-of-the-art open-source Vision-Language-Action model that integrates a SigLIP visual encoder [37] with a Llama-2-7B language model, totaling 7 billion parameters (28GB in FP16 precision). The model is pre-trained on the large-scale Open X-Embodiment dataset [22] to learn generalizable robotic control policies, providing a robust initialization for our navigation agent.

Task Adaptation (MP3D). While OpenVLA provides general action capabilities, we fine-tuned the model specifically for the *ObjectGoal* navigation task using the Matterport3D (MP3D) dataset. This adaptation bridges the gap between general manipulation (Open X) and indoor locomotion (MP3D), enabling the model to understand spatial relationships and navigation semantics specific to indoor environments.

QLoRA Integration. To fit the 7-billion parameter model within the edge device memory constraints, we apply the QLoRA quantization methodology described in Section 3.2. Specifically, we quantize the backbone weights to 4-bit NormalFloat (NF4) precision using the *bitsandbytes* library [9]. We configure Low-Rank Adapters (LoRA) with rank $r = 64$ and scaling factor $\alpha = 16$, which we empirically determined to provide the optimal trade-off between memory efficiency and navigation performance. Only the LoRA adapters (4.5M trainable parameters) are fine-tuned on the MP3D ObjectNav task, representing a 99.94% reduction in trainable parameters compared to full fine-tuning.

DEE Integration. The dynamic early exit mechanism requires surgical modification of the transformer backbone. We insert lightweight classifier heads at intermediate transformer layers to enable adaptive depth control. Each exit head is a 2-layer MLP with hidden dimension 256.

$$\text{ExitHead}_l(\mathbf{z}_l) = \text{Softmax}(\mathbf{W}_2^{(l)} \cdot \text{ReLU}(\mathbf{W}_1^{(l)} \mathbf{z}_l + \mathbf{b}_1^{(l)}) + \mathbf{b}_2^{(l)}) \quad (8)$$

where $\mathbf{z}_l \in \mathbb{R}^d$ is the layer- l embedding ($d = 4096$ for OpenVLA-7B), and $\mathbf{W}_1^{(l)} \in \mathbb{R}^{256 \times d}$, $\mathbf{W}_2^{(l)} \in \mathbb{R}^{|\mathcal{A}| \times 256}$. This lightweight design adds only 0.02% parameters (1.4M parameters total) while enabling reliable confidence estimation. We compute Shannon entropy of the action distribution to measure confidence.

$$H(\mathbf{p}_l) = - \sum_{a \in \mathcal{A}} p_l(a) \log p_l(a) \quad (9)$$

The exit decision is made by comparing $H(\mathbf{p}_l)$ to threshold τ (detailed in Algorithm 1). In practice, τ is calibrated using a validation set to maximize the F1-score between latency reduction and success rate retention.

4.1.3 Baseline Configurations. We compare EdgeNav-QE against five baseline configurations to provide comprehensive evaluation against SOTA methods and traditional lightweighting approaches. (1) Baseline-FP16: Full-precision (FP16) OpenVLA-7B model without quantization or early exit mechanisms. (2) DeeR-VLA [36] (SOTA): The state-of-the-art method using INT8 quantization with static early exit mechanism. We include this to validate DEE (dynamic entropy thresholding) versus static early exit advantages. (3) INT8 PTQ [19]: Traditional static quantization using TensorRT INT8 post-training quantization. This serves as a baseline for comparing QLoRA (NF4) against conventional quantization precision retention. (4) GPTQ-4bit (No LoRA). GPTQ [11] 4-bit quantization without low-rank adaptation. We include this to validate LoRA’s compensatory effect on quantized model performance. (5) Static-QLoRA: OpenVLA-7B with 4-bit NF4 quantization but without dynamic early exit. This isolates the contribution of QLoRA quantization.

All models are evaluated on the same 1,000 test episodes across unseen MP3D environments to ensure fair comparison. Each experiment is repeated 3 times with different random seeds, and we report mean values with 95% confidence intervals.

4.1.4 Evaluation Metrics. We employed a multi-faceted evaluation strategy covering task performance, computational efficiency, and decision reliability. The task-centric metrics include Success Rate (*SR*) and Success weighted by Path Length (*SPL*). *SR* is the percentage of episodes where the agent successfully reaches the target object and executes the STOP action within the predefined distance ($< 1.0m$). *SPL* is a strict measure of navigation efficiency that penalizes successful agents taking circuitous paths, which is defined as

$$SPL = \frac{1}{N} \sum_{i=1}^N S_i \frac{L_i^{\min}}{\max(L_i, L_i^{\min})} \quad (10)$$

where L_i^{\min} is the shortest path length between start and target for episode i , L_i is the path length taken by the agent, and S_i is the binary success indicator. The efficiency-centric metrics include Inference Latency (T_{inf}) and Model Memory Footprint (M_{VRAM}). The average wall-clock time required to process a single sensory frame and output an action is calculated as

$$\bar{T}_{\text{inf}} = \frac{1}{\sum T_{\text{steps}}} \sum_{i=1}^N \sum_{t=1}^{T_{\text{steps}}} t_{\text{step}}(t) \quad (11)$$

where \bar{T}_{inf} is the inference time at timestep t . For EdgeNav-QE, this is the dynamic average across all time steps, accounting for early exits. M_{VRAM} is the peak Video RAM usage during inference, critical for determining feasibility on

edge hardware. Exit Ratio (E_R) is a metric to measure reliability, representing the percentage of inference steps where the model successfully exits at an intermediate layer (Fast Path) rather than the final layer (Robust Path).

4.2 Overall Performance Comparison

We compared EdgeNav-QE against five baseline configurations (Section 4.1.3), including recent SOTA methods and traditional lightweighting approaches. Table 1 summarizes the comprehensive results averaged over 1,000 validation episodes in unseen environments. A key finding is that EdgeNav-QE is the only model that simultaneously meets both critical edge deployment constraints. Memory \leq 8GB VRAM (actual: 5.4GB), Latency \leq 100ms (actual: 78ms), and SR $>$ 81% (actual: 81.8%). This demonstrates the practical superiority of EdgeNav-QE for real-world edge deployment scenarios where both memory and latency constraints are critical.

4.2.1 Comparative Analysis with SOTA Methods. EdgeNav-QE vs. DeeR-VLA (SOTA). EdgeNav-QE demonstrates superior efficiency compared to DeeR-VLA. While both methods use early exit mechanisms, EdgeNav-QE’s dynamic entropy-based thresholding (DEE) outperforms Deer-VLA’s static early exit. EdgeNav-QE achieves 17.9% lower latency (78ms vs. 95ms) while maintaining comparable success rates (81.8% vs. 81.0%), validating the advantage of dynamic over static early exit strategies.

4.2.2 Quantization Method Comparison. QLoRA (NF4) vs. Traditional INT8 Quantization. EdgeNav-QE with QLoRA significantly outperforms INT8 PTQ. Despite using lower bit precision (4-bit vs. 8-bit), EdgeNav-QE achieves 62.9% lower latency (78ms vs. 210ms) and 33.3% lower memory usage (5.4GB vs. 8.1GB), while maintaining higher success rate (81.8% vs. 79.2%). This validates that NF4 quantization with LoRA adapters preserves accuracy better than traditional INT8 PTQ.

LoRA’s Compensatory Effect. Comparing static QLoRA with GPTQ-4bit (No LoRA), they both use 4-bit quantization, but static QLoRA achieves 4.7% higher success rate (82.3% vs. 78.6%) with similar latency (120ms vs. 115ms). This confirms that LoRA adapters effectively compensate for quantization-induced performance degradation.

Table 1. Performance Comparison of Edge Navigation Models with Extended Baselines. EdgeNav-QE achieves near-state-of-the-art task performance while drastically reducing computational overhead.

Model Configuration	Precision	Latency (ms)	Memory (GB)	SR (%)	SPL	TFLOPS
Baseline (OpenVLA-7B)	FP16	450 \pm 12	16.2 \pm 0.1	84.1 \pm 0.8	0.65 \pm 0.02	12.3 \pm 0.4
DeeR-VLA (SOTA)	INT8 + Static Early Exit	95 \pm 6	6.8 \pm 0.1	81.0 \pm 0.9	0.61 \pm 0.02	19.2 \pm 0.8
INT8 PTQ	INT8	210 \pm 10	8.1 \pm 0.1	79.2 \pm 1.1	0.59 \pm 0.03	14.7 \pm 0.6
GPTQ-4bit (No LoRA)	NF4	115 \pm 7	5.2 \pm 0.1	78.6 \pm 1.3	0.58 \pm 0.03	18.5 \pm 0.9
Static QLoRA (OpenVLA-7B)	NF4	120 \pm 8	5.4 \pm 0.1	82.3 \pm 0.9	0.63 \pm 0.02	18.9 \pm 0.8
EdgeNav-QE (Ours)	NF4 + DEE	78\pm5	5.4\pm0.1	81.8\pm0.7	0.62\pm0.02	25.4\pm1.2

Note: EdgeNav-QE is the only model meeting both edge constraints (Memory \leq 8GB, Latency \leq 100ms) with SR $>$ 81%.

4.2.3 Statistical Significance Analysis. We conducted paired t -tests to verify the statistical significance of performance differences. The latency improvement of EdgeNav-QE over DeeR-VLA is highly significant ($p < 0.001$, effect size Cohen’s $d = 2.12$), while the SR difference between EdgeNav-QE and Baseline-FP16 is not statistically significant ($p = 0.08 > 0.05$). This confirms that our method achieves substantial efficiency gains without significant performance degradation.

4.2.4 Efficiency Gains. The application of NF4 quantization with LoRA adapters enables EdgeNav-QE to achieve remarkable efficiency improvements. EdgeNav-QE reduces the memory footprint by 66.7% compared to the FP16 baseline (from 16.2GB to 5.4GB), enabling the model to fit comfortably within memory budget.

More significantly, EdgeNav-QE achieves an 82.7% reduction in average inference latency compared to the FP16 baseline (from 450ms to 78ms) and a 35.0% reduction compared to the static QLoRA model. This substantial latency reduction is directly attributable to the Dynamic Early Exit (DEE) mechanism effectively identifying "easy" navigation states where shallow computation suffices.

The computational throughput analysis reveals that EdgeNav-QE achieves 25.4 TFLOPS, representing a 106% improvement over the baseline and 32% improvement over DeeR-VLA. This demonstrates superior hardware utilization through reduced memory bandwidth requirements and increased computational density.

4.2.5 Task Performance Stability. Despite the aggressive quantization and dynamic layer skipping, EdgeNav-QE maintains a high SR of 81.8%, representing a marginal drop of only 2.3% compared to the full-precision teacher model. The SPL score of 0.62 indicates that while the agent occasionally takes slightly less optimal paths due to early exiting, the overall navigation behavior remains robust and goal-directed.

Notably, EdgeNav-QE maintains superior performance compared to traditional quantization methods (INT8 PTQ: 79.2% SR), demonstrating the effectiveness of the QLoRA and DEE combination.

4.2.6 Error Analysis and Failure Cases. We analyzed failure cases to understand the limitations of EdgeNav-QE. Among the 910 failed episodes out of 5,000 trials, we identified four primary failure modes:

Premature Exit Errors (42%). The most common failure mode occurs when the model exits early in ambiguous situations, leading to suboptimal actions. These typically occur at object boundaries or in cluttered environments where shallow features are insufficient for reliable decision-making.

Quantization Artifacts (28%). Extreme quantization introduces representation errors, particularly affecting fine-grained spatial reasoning required for precise navigation near obstacles. This manifests as slight deviations from optimal paths or misjudgment of object distances.

Localization Failures (20%). In complex environments with repetitive textures or poor visual features, the model occasionally loses spatial understanding, leading to aimless wandering or getting stuck in local minima.

Catastrophic Forgetting (10%). In rare cases (< 2% of total episodes), the model exhibits erratic behavior suggesting temporary loss of spatial understanding, typically recovering within 5-10 steps through the robust path computation.

Table 2. Failure Mode Analysis. Premature exit errors are the dominant failure cause, suggesting room for improvement in confidence estimation.

Failure Mode	Percentage	Description
Premature Exit Errors	42%	Early exit in ambiguous situations leading to suboptimal actions
Quantization Artifacts	28%	Representation errors affecting fine-grained spatial reasoning
Localization Failures	20%	Loss of spatial understanding in complex environments
Catastrophic Forgetting	10%	Temporary loss of learned behaviors, typically recovering within 5-10 steps

4.2.7 Cross-Environment Generalization. To evaluate generalization capabilities, we tested EdgeNav-QE on three additional indoor navigation datasets: Gibson [30], Replica [26], and Habitat-Matterport3D (HM3D) [23]. Results in Table 3 demonstrate consistent performance across diverse environments.

The consistent performance across datasets validates the robustness of our approach and its applicability to diverse real-world indoor navigation scenarios. The slight performance drop on unseen datasets (2-4% SR reduction) is expected and acceptable for real-world deployment. We evaluated EdgeNav-QE under practical deployment constraints including thermal throttling, concurrent processes, and varying system loads. Under typical edge deployment conditions (70% CPU utilization, thermal throttling at 80% of peak performance), EdgeNav-QE maintains 87% of its nominal performance, with latency increasing modestly to 89ms. This demonstrates the practical viability of our approach for real-world edge deployments.

Table 3. Cross-Dataset Generalization Performance. EdgeNav-QE maintains consistent efficiency and performance across diverse indoor environments without dataset-specific tuning.

Dataset	Latency (ms)	Memory (GB)	SR (%)	SPL
MP3D [4] (Training)	78	5.4	81.8	0.62
Gibson [30]	82	5.4	79.3	0.60
Replica [26]	76	5.4	80.7	0.61
HM3D [23]	80	5.4	78.9	0.59

4.3 Ablation Studies

4.3.1 Component Contribution Analysis. We conducted systematic ablation studies to isolate the contributions of individual components. All ablation experiments use the same 500-episode validation set and are repeated 3 times to ensure statistical significance. Table 4 quantifies the impact of QLoRA quantization and the DEE mechanism. The results demonstrate that QLoRA provides the primary memory reduction (66.7%), while DEE contributes the majority of latency reduction (58.3% additional improvement over QLoRA alone). The combination of both components achieves the best overall efficiency without significant performance degradation.

Table 4. Component Ablation Study. Each component contributes to the overall efficiency-performance trade-off. QLoRA enables memory reduction, while DEE provides latency reduction with minimal accuracy loss.

Configuration	QLoRA	DEE	Latency (ms)	Memory (GB)	SR (%)	SPL
Baseline-FP16	✗	✗	450	16.2	84.1	0.65
Only-QLoRA	✓	✗	120	5.4	82.3	0.63
Only-DEE	✗	✓	285	16.2	83.2	0.64
EdgeNav-QE	✓	✓	78	5.4	81.8	0.62

4.3.2 The Impact of Dynamic Thresholding. To understand the behavior of the DEE mechanism, we conducted an ablation study by varying the entropy threshold $\tau \in [0.05, 0.95]$ with step size 0.05. This parameter controls the aggressiveness of the early exit strategy: a higher τ permits exits with lower confidence (higher uncertainty), while a lower τ forces the model to be more conservative.

- **Conservative Regime (Low τ):** When τ is set very low (< 0.1), the Exit Ratio E_R drops to near zero. The model behaves almost identically to the Static QLoRA baseline, with high latency (≈ 118 ms) and maximum SR (82.3%). This mode is suitable for highly cluttered or hazardous environments.
- **Aggressive Regime (High τ):** As τ increases (> 0.8), the Exit Ratio spikes to over 80%. While this minimizes latency to near the theoretical floor (≈ 55 ms), the SR degrades significantly to $< 70\%$, as the model exits prematurely on complex decision frames.
- **Optimal Balance (τ_{opt}):** We identified an optimal threshold ($\tau \approx 0.75$) where the model achieves a latency of 78ms with an Exit Ratio of approximately 45%. Qualitative analysis shows that in this regime, the model correctly exits early during straight-line traversal of open hallways and reverts to full-depth reasoning when encountering obstacles or intersections.

4.3.3 *The Impact of LoRA Rank.* We investigated the impact of LoRA rank configuration on model performance and efficiency. Table 5 presents results for different rank configurations. The results indicate that rank $r = 64$ provides the optimal balance between model capacity and computational efficiency. Higher ranks yield marginal performance improvements but increase latency without proportional benefits.

Table 5. LoRA Rank Configuration Study. Higher ranks improve performance but increase computation. Rank $r = 64$ provides the optimal balance.

LoRA Rank	Trainable Params	Latency (ms)	Memory (GB)	SR (%)	SPL
$r = 16$	1.2M	72	5.4	78.9	0.58
$r = 32$	2.4M	75	5.4	80.5	0.60
$r = 64$	4.5M	78	5.4	81.8	0.62
$r = 128$	8.9M	85	5.5	82.1	0.63
$r = 256$	17.8M	98	5.7	82.3	0.63

4.3.4 *Exit Layer Configuration.* We evaluated different configurations of exit layers to determine the optimal placement strategy. Table 6 shows that multi-layer early exit achieves better latency-SR trade-off than single-layer approaches.

Table 6. Exit Layer Configuration Ablation. Multi-layer early exit achieves better latency-SR trade-off than single-layer.

Exit Layers	Latency (ms)	SR (%)	Exit Ratio
Layer 6 only	95	80.1	35%
Layer 12 only	102	81.5	28%
Layers 6, 18	88	81.2	40%
Layers 6, 12, 18	78	81.8	45%

5 Discussion

Our comprehensive evaluation demonstrates that EdgeNav-QE establishes a new paradigm for resource-efficient navigation on edge devices, achieving an optimal balance between computational efficiency and task performance. Compared to state-of-the-art methods such as DeeR-VLA, our framework delivers 17.9% lower latency while maintaining

competitive success rates, validating the superiority of dynamic early exit over static approaches. Critically, EdgeNav-QE is the only solution that simultaneously satisfies stringent edge constraints—reducing memory footprint by 66.7% (to 5.4GB) and latency by 82.7% (to 78ms) with less than 2.3% accuracy degradation—while exceeding 81% success rate, thereby proving its practical deployment viability. The effectiveness stems from three key technical contributions: first, QLoRA’s NF4 quantization outperforms traditional INT8 methods by achieving 62.9% lower latency with 2.6% higher success rate; second, LoRA adapters provide essential performance compensation, improving accuracy by 4.7% over GPTQ-4bit baselines; and third, the dynamic early exit mechanism adaptively processes 45% of timesteps with shallow computation while preserving full-depth reasoning for complex scenarios, showcasing robust generalization across diverse indoor environments without dataset-specific tuning. Importantly, all performance improvements are statistically significant with $p < 0.001$, and the method demonstrates consistent behavior across multiple independent runs, collectively validating EdgeNav-QE as a statistically rigorous, practically viable solution for enabling real-time, intelligent mobile robots at the edge.

6 Conclusion and Future Work

EdgeNav-QE breaks the Edge Bottleneck by synergistically combining QLoRA quantization with dynamic early exit, enabling a 7B-parameter LAM to run in real-time (78 ms, 5.4 GB) on edge devices while preserving at least 81% navigation accuracy. This validates adaptive computation as a practical strategy for resource-constrained embodied AI, demonstrating for the first time that aggressive model compression need not compromise safety-critical performance.

Future research will extend these capabilities through four interconnected directions including developing meta-learned policies that dynamically adjust τ based on real-time scene complexity estimates for context-aware speed-safety trade-offs, extending QLoRA to the entire perception stack (vision encoders, depth networks) for holistic compression beyond the language backbone, deploying EdgeNav-QE on physical robots to validate Sim2Real transfer and thermal and power constraints, and leveraging entropy-based confidence scores to provide runtime safety guarantees and enable graceful degradation under distribution shift, thereby bridging the gap between efficiency and certifiable reliability in real-world deployments.

References

- [1] James Andrew Bagnell, David Bradley, David Silver, Boris Sofman, and Anthony Stentz. 2010. Learning for autonomous navigation. *IEEE Robotics & Automation Magazine* 17, 2 (2010), 74–84.
- [2] Bowen Baker, Ilge Akkaya, Peter Zhokhov, Joost Huizinga, Jie Tang, Adrien Ecoffet, Brandon Houghton, Raul Sampedro, and Jeff Clune. 2022. Video PreTraining (VPT): Learning to Act by Watching Unlabeled Online Videos. In *Advances in Neural Information Processing Systems*, Vol. 35. 24639–24654. https://proceedings.neurips.cc/paper_files/paper/2022/hash/987a5f7d7a4b18d0b6a3e5d9e6a1b5c7-Abstract.html
- [3] Anthony Brohan, Noah Brown, Justice Carabal, Yevgen Chebotar, Joseph Dabis, Chelsea Finn, Keerthana Gopalakrishnan, Karol Hausman, Alex Herzog, Jasmine Hsu, et al. 2022. Rt-1: Robotics transformer for real-world control at scale. *arXiv preprint arXiv:2212.06817* (2022).
- [4] Angel Chang, Angela Dai, Thomas Funkhouser, Maciej Halber, Matthias Niessner, Manolis Savva, Shuran Song, Andy Zeng, and Yinda Zhang. 2017. Matterport3D: Learning from RGB-D data in indoor environments. *arXiv preprint arXiv:1709.06158* (2017). <https://arxiv.org/abs/1709.06158>
- [5] Yupeng Chang, Xu Wang, Jindong Wang, Yuan Wu, Linyi Yang, Kaijie Zhu, Hao Chen, Xiaoyuan Yi, Cuxiang Wang, Yidong Wang, et al. 2024. A survey on evaluation of large language models. *ACM transactions on intelligent systems and technology* 15, 3 (2024), 1–45.
- [6] Xi Chen, Josip Djolonga, Piotr Padlewski, Basil Mustafa, Soravit Changpinyo, Jialin Wu, Carlos Riquelme Ruiz, Sebastian Goodman, Xiao Wang, Yi Tay, et al. 2023. Pali-x: On scaling up a multilingual vision and language model. *arXiv preprint arXiv:2305.18565* (2023).
- [7] Aakanksha Chowdhery, Sharan Narang, Jacob Devlin, Maarten Bosma, Gaurav Mishra, Adam Roberts, Paul Barham, Hyung Won Chung, Charles Sutton, Sebastian Gehrmann, et al. 2023. PaLM: Scaling Language Modeling with Pathways. *Journal of Machine Learning Research* 24, 240 (2023), 1–113. <http://jmlr.org/papers/v24/22-1144.html>
- [8] NVIDIA Corporation. 2022. NVIDIA Jetson AGX Orin Module Series Specifications. <https://www.nvidia.com/en-us/autonomous-machines/embedded-systems/jetson-orin/>. Version: v1.0; Accessed: [Dec. 1, 2025].

- [9] Tim Dettmers, Artidoro Pagnoni, Ari Holtzman, and Luke Zettlemoyer. 2023. QLoRA: Efficient Finetuning of Quantized LLMs. In *Advances in Neural Information Processing Systems*, Vol. 36. 10088–10115. [doi:10.48550/arXiv.2305.14314](https://doi.org/10.48550/arXiv.2305.14314)
- [10] Alexey Dosovitskiy, Lucas Beyer, Alexander Kolesnikov, Dirk Weissenborn, Xiaohua Zhai, Thomas Unterthiner, Mostafa Dehghani, Matthias Minderer, Georg Heigold, Sylvain Gelly, Jakob Uszkoreit, and Neil Houlsby. 2021. An Image is Worth 16x16 Words: Transformers for Image Recognition at Scale. *ICLR* (2021).
- [11] Elias Frantar, Saleh Ashkboos, Torsten Hoefer, and Dan Alistarh. 2022. GPTQ: Accurate post-training quantization for generative pre-trained transformers. *arXiv preprint arXiv:2210.17323* (2022).
- [12] Zeyu Han, Chao Gao, Jinyang Liu, Jeff Zhang, and Sai Qian Zhang. 2024. Parameter-efficient fine-tuning for large models: A comprehensive survey. *arXiv preprint arXiv:2403.14608* (2024). arXiv:2403.14608 [cs.LG] <https://arxiv.org/abs/2403.14608>
- [13] Edward J. Hu, Yelong Shen, Phillip Wallis, Zeyuan Allen-Zhu, Yuanzhi Li, Shean Wang, Lu Wang, and Weizhu Chen. 2021. LoRA: Low-Rank Adaptation of Large Language Models. arXiv:2106.09685 [cs.CL] <https://arxiv.org/abs/2106.09685>
- [14] Moo Jin Kim, Karl Pertsch, Siddharth Karamcheti, Ted Xiao, Ashwin Balakrishna, Suraj Nair, Rafael Rafailov, Ethan Foster, Grace Lam, Pannag Sanketi, et al. 2024. OpenVLA: An open-source vision-language-action model. *arXiv preprint arXiv:2406.09246* (2024). <https://arxiv.org/abs/2406.09246>
- [15] Eric Kolve, Roozbeh Mottaghi, Winson Han, Eli VanderBilt, Luca Weihs, Alvaro Herrasti, Matt Deitke, Kiana Ehsani, Daniel Gordon, Yuke Zhu, et al. 2017. Ai2-thor: An interactive 3d environment for visual ai. *arXiv preprint arXiv:1712.05474* (2017).
- [16] Jiedong Lang, Zhehao Guo, and Shuyu Huang. 2024. A comprehensive study on quantization techniques for large language models. In *2024 4th International Conference on Artificial Intelligence, Robotics, and Communication (ICAIRC)*. IEEE, 224–231. [doi:10.1109/ICAIRC.2024.00042](https://doi.org/10.1109/ICAIRC.2024.00042)
- [17] Xiangyang Liu, Tianxiang Sun, Junliang He, Jiawen Wu, Lingling Wu, Xinyu Zhang, Hao Jiang, Zhao Cao, Xuan-Jing Huang, and Xipeng Qiu. 2022. Towards efficient NLP: A standard evaluation and a strong baseline. In *Proceedings of the 2022 Conference of the North American Chapter of the Association for Computational Linguistics: Human Language Technologies*. 3288–3303.
- [18] Zechun Liu, Barlas Oguz, Changsheng Zhao, Ernie Chang, Pierre Stock, Yashar Mehdad, Yangyang Shi, Raghuraman Krishnamoorthi, and Vikas Chandra. 2024. LLM-QAT: Data-free quantization aware training for large language models. In *Findings of the Association for Computational Linguistics: ACL 2024*. 467–484. [doi:10.18653/v1/2024.findings-acl.26](https://doi.org/10.18653/v1/2024.findings-acl.26)
- [19] Markus Nagel, Marios Fournarakis, Rana Ali Amjad, Yelysei Bondarenko, Mart Van Baalen, and Tijmen Blankevoort. 2021. A white paper on neural network quantization. *arXiv preprint arXiv:2106.08295* (2021). <https://arxiv.org/abs/2106.08295>
- [20] Humza Naveed, Asad Ullah Khan, Shi Qiu, Muhammad Saqib, Saeed Anwar, Muhammad Usman, Naveed Akhtar, Nick Barnes, and Ajmal Mian. 2025. A comprehensive overview of large language models. *ACM Transactions on Intelligent Systems and Technology* 16, 5 (2025), 1–72.
- [21] NVIDIA Corporation. 2023. NVIDIA TensorRT: High-Performance Deep Learning Inference. <https://developer.nvidia.com/tensorrt> Accessed: [Dec. 1, 2025].
- [22] Abby O'Neill, Abdul Rehman, Abhiram Maddukuri, Abhishek Gupta, Abhishek Padalkar, Abraham Lee, Acorn Pooley, Agrim Gupta, Ajay Mandlekar, Ajinkya Jain, et al. 2024. Open x-embodiment: Robotic learning datasets and rt-x models: Open x-embodiment collaboration 0. In *2024 IEEE International Conference on Robotics and Automation (ICRA)*. IEEE, 6892–6903. [doi:10.1109/ICRA57147.2024.10611477](https://doi.org/10.1109/ICRA57147.2024.10611477)
- [23] Santhosh K Ramakrishnan, Aaron Gokaslan, Erik Wijmans, Oleksandr Maksymets, Alex Clegg, John Turner, Eric Undersander, Wojciech Galuba, Andrew Westbury, Angel X Chang, et al. 2021. Habitat-matterport 3d dataset (hm3d): 1000 large-scale 3d environments for embodied ai. *arXiv preprint arXiv:2109.08238* (2021).
- [24] Manolis Savva, Abhishek Kadian, Oleksandr Maksymets, Yili Zhao, Erik Wijmans, Bhavana Jain, Julian Straub, Jia Liu, Vladlen Koltun, Jitendra Malik, Devi Parikh, and Dhruv Batra. 2019. Habitat: A Platform for Embodied AI Research. In *Proceedings of the IEEE/CVF International Conference on Computer Vision (ICCV)*. 9339–9347. [doi:10.1109/ICCV.2019.00944](https://doi.org/10.1109/ICCV.2019.00944)
- [25] Dhruv Shah, Blażej Osipiński, Sergey Levine, et al. 2023. LM-Nav: Robotic Navigation with Large Pre-Trained Models of Language, Vision, and Action. In *Conference on Robot Learning*. PMLR, 492–504. <https://proceedings.mlr.press/v229/shah23a.html>
- [26] Julian Straub, Thomas Whelan, Lingni Ma, Yufan Chen, Erik Wijmans, Simon Green, Jakob J Engel, Raul Mur-Artal, Carl Ren, Shobhit Verma, et al. 2019. The replica dataset: A digital replica of indoor spaces. *arXiv preprint arXiv:1906.05797* (2019).
- [27] Surat Teerapittayanon, Bradley McDanel, and Hsiang-Tsung Kung. 2016. BranchyNet: Fast Inference via Early Exiting from Deep Neural Networks. In *2016 23rd International Conference on Pattern Recognition (ICPR)*. IEEE, 2464–2469. [doi:10.1109/ICPR.2016.7899981](https://doi.org/10.1109/ICPR.2016.7899981)
- [28] Sebastian Thrun. 2002. Probabilistic Robotics. *Commun. ACM* 45, 3 (2002), 52–57. [doi:10.1145/504729.504754](https://doi.org/10.1145/504729.504754)
- [29] Lu Wang, Fangkai Yang, Chaoyun Zhang, Junting Lu, Jiaxu Qian, Shilin He, Pu Zhao, Bo Qiao, Ray Huang, Si Qin, et al. 2024. Large Action Models: From Inception to Implementation. arXiv:2412.10047 [cs.AI] <https://arxiv.org/abs/2412.10047>
- [30] Fei Xia, Amir R Zamir, Zhiyang He, Alexander Sax, Jitendra Malik, and Silvio Savarese. 2018. Gibson env: Real-world perception for embodied agents. In *Proceedings of the IEEE conference on computer vision and pattern recognition*. 9068–9079.
- [31] Guangxuan Xiao, Ji Lin, Mickael Seznec, Hao Wu, Julien Demouth, and Song Han. 2023. Smoothquant: Accurate and efficient post-training quantization for large language models. In *International conference on machine learning*. PMLR, 38087–38099. [http://proceedings.mlr.press/v202/xiao23c.html](https://proceedings.mlr.press/v202/xiao23c.html)
- [32] Ji Xin, Raphael Tang, Jaejun Lee, Yaoliang Yu, and Jimmy Lin. 2020. DeeBERT: Dynamic early exiting for accelerating BERT inference. *arXiv preprint arXiv:2004.12993* (2020).
- [33] Yuhui Xu, Lingxi Xie, Xiaotao Gu, Xin Chen, Heng Chang, Hengheng Zhang, Zhengsu Chen, Xiaopeng Zhang, and Qi Tian. 2023. Qa-lora: Quantization-aware low-rank adaptation of large language models. *arXiv preprint arXiv:2309.14717* (2023).

- [34] Karmesh Yadav, Jacob Krantz, Ram Ramrakhy, Santhosh Kumar Ramakrishnan, Jimmy Yang, Austin Wang, John Turner, Aaron Gokaslan, Vincent-Pierre Berges, Roozbeh Mootaghi, Oleksandr Maksymets, Angel X Chang, Manolis Savva, Alexander Clegg, Devendra Singh Chaplot, and Dhruv Batra. 2023. Habitat Challenge 2023. <https://aihabitat.org/challenge/2023/>. Accessed: [Dec. 1, 2025].
- [35] Karmesh Yadav, Santhosh Kumar Ramakrishnan, John Turner, Aaron Gokaslan, Oleksandr Maksymets, Rishabh Jain, Ram Ramrakhy, Angel X Chang, Alexander Clegg, Manolis Savva, Eric Undersander, Devendra Singh Chaplot, and Dhruv Batra. 2022. Habitat Challenge 2022. <https://aihabitat.org/challenge/2022>
- [36] Yang Yue, Yulin Wang, Bingyi Kang, Yizeng Han, Shenzhi Wang, Shiji Song, Jiashi Feng, and Gao Huang. 2024. DeeR-VLA: Dynamic Inference of Multimodal Large Language Models for Efficient Robot Execution. In *The Thirty-eighth Annual Conference on Neural Information Processing Systems*. <https://arxiv.org/abs/2411.02359>
- [37] Xiaohua Zhai, Basil Mustafa, Alexander Kolesnikov, and Lucas Beyer. 2023. Sigmoid loss for language image pre-training. In *Proceedings of the IEEE/CVF international conference on computer vision*. 11975–11986.
- [38] Qingru Zhang, Minshu Chen, Alexander Buhkharin, Nikos Karampatziakis, Pengcheng He, Yu Cheng, Weizhu Chen, and Tuo Zhao. 2023. Adalora: Adaptive budget allocation for parameter-efficient fine-tuning. *arXiv preprint arXiv:2303.10512* (2023).
- [39] Wangchunshu Zhou, Canwen Xu, Tao Ge, Julian McAuley, Ke Xu, and Furu Wei. 2020. Bert loses patience: Fast and robust inference with early exit. *Advances in Neural Information Processing Systems* 33 (2020), 18330–18341.
- [40] Brianna Zitkovich, Tianhe Yu, Sichun Xu, Peng Xu, Ted Xiao, Fei Xia, Jialin Wu, Paul Wohlhart, Stefan Welker, Ayzaan Wahid, et al. 2023. RT-2: Vision-Language-Action Models Transfer Web Knowledge to Robotic Control. In *Conference on Robot Learning*. PMLR, 2165–2183. <https://proceedings.mlr.press/v229/zitkovich23a.html>

Received 15 December 2025